Biochimica et Biophysica Acta 1833 (2013) 593–601

Contents lists available at SciVerse ScienceDirect

Biochimica et Biophysica Acta

journal homepage: www.elsevier.com/locate/bbamcr

Lack of Sir2 increases acetate consumption and decreases extracellular pro-aging factors

Nadia Casatta [1], Alessandra Porro [1], Ivan Orlandi, Luca Brambilla, Marina Vai *

Dipartimento di Biotecnologie e Bioscienze, Università di Milano-Bicocca, Piazza della Scienza 2, 20126 Milano, Italy

ARTICLE INFO

Article history:
Received 26 March 2012
Received in revised form 5 November 2012
Accepted 8 November 2012
Available online 16 November 2012

Keywords:
Chronological aging
Sir2
Acetate metabolism
Acetyl-CoA
Ethanol
Gluconeogenesis

ABSTRACT

Yeast chronological aging is regarded as a model for aging of mammalian post-mitotic cells. It refers to changes occurring in stationary phase cells over a relatively long period of time. How long these cells can survive in such a non-dividing state defines the chronological lifespan. Several factors influence cell survival including two well known normal by-products of yeast glucose fermentation such as ethanol and acetic acid. In fact, the presence in the growth medium of these C2 compounds has been shown to limit the chronological lifespan. In the chronological aging paradigm, a pro-aging role has also emerged for the deacetylase Sir2, the founding member of the Sirtuin family, whose loss of function increases the depletion of extracellular ethanol by an unknown mechanism. Here, we show that lack of Sir2 strongly influences carbon metabolism. In particular, we point out a more efficient acetate utilization which in turn may have a stimulatory effect on ethanol catabolism. This correlates with an enhanced glyoxylate/gluconeogenic flux which is fuelled by the acetyl-CoA produced from the acetate activation. Thus, when growth relies on a respiratory metabolism such as that on ethanol or acetate, *SIR2* inactivation favors growth. Moreover, in the chronological aging paradigm, the increase in the acetate metabolism implies that *sir2Δ* cells avoid acetic acid accumulation in the medium and deplete ethanol faster; consequently pro-aging extracellular signals are reduced. In addition, an enhanced gluconeogenesis allows replenishment of intracellular glucose stores which may be useful for better long-term cell survival.

1. Introduction

Aging is a time-dependent progressive and irreversible physiological/functional decline of an organism that is accompanied by an increased vulnerability to both environmental stress and diseases and increased risk of mortality. On the whole, aging is a complex multi-factorial process modulated by interplay between genetic and environmental factors. No single variable can adequately capture the full extent of this complexity since several processes interact simultaneously and operate at different levels of functional organization [1,2]. The budding yeast *Saccharomyces cerevisiae* is one of the most established model systems used for aging-related research which provides, among others, the opportunity to study and compare the aging processes of both proliferating and non-proliferating cells in a simple single-celled organism. In fact, in yeast two aging paradigms have been described: replicative and chronological. In the former, replicative lifespan (RLS) is defined as the number of daughter cells an asymmetrically dividing mother generates in the presence of nutrients before senescence [3]. In the latter, chronological lifespan (CLS) is the mean and maximum survival period of a population of non-dividing cells in stationary phase. Viability over time, in this case, is defined as the ability to resume mitotic growth upon return to rich fresh medium [4]. In the stationary phase, yeast cells display a survival-based metabolism and acquire physiological and morphological features, including a thickened cell wall, accumulation of storage carbohydrates and increased stress resistance, which result from the integrated responses of different signalling pathways. The establishment of a quiescent program allows the cells to survive starvation and resume growth when nutrient conditions become favorable again [5]. CLS can be extended by either inhibition/reduced activity of two major nutrient-sensing pathways such as TORC1-Sch9 and Ras-PKA ones, or by calorie restriction (CR), the practice of limiting nutrient intake which in yeast is generally imposed by reducing the glucose concentration in the growth medium [6–8]. Defects in TORC1-Sch9 or Ras-PKA signaling as well as CR lead to in part common downstream targets (Rim15, Msn2/4 and Gis1) which ultimately by increasing endogenous stress defence mechanisms contribute to enhance cell survival [6,9]. Moreover, during chronological aging, in addition to the well known intrinsic factors such as hydrogen peroxide and superoxide [10], cellular stresses also include extrinsic factors such as ethanol and acidic acid. In fact, in some settings, the presence in the growth medium of these two by-products of the yeast metabolism restricts CLS [11,12].

In the chronological aging paradigm, a pro-aging role is also played by Sir2 [12]. Sir2 is the founding member of Sirtuins, a family which comprises the unique class III of NAD^+-dependent deacetylases

* Corresponding author. Tel.: +39 0264483531; fax: +39 0264483565.
E-mail address: marina.vai@unimib.it (M. Vai).
[1] These authors contributed equally to this work.

0167-4889/$ – see front matter © 2012 Elsevier B.V. All rights reserved.
http://dx.doi.org/10.1016/j.bbamcr.2012.11.008

known to be evolutionary conserved regulators of aging [1,7,13]. Much work in yeast has focused on histone deacetylation, but a wide range of non-chromatin substrates for the other Sirtuins have been identified which are involved in different metabolic processes including energy production, the urea cycle, fatty acid and acetate metabolism [14,15]. Concerning the acetate metabolism, in mammals, acetate derived from both exogenous and endogenous sources, is activated to acetyl-CoA either in the cytoplasm by acetyl-CoA synthetase 1 (AceCS1) or in the mitochondria by AceCS2 [16,17]. The Sirtuins, SIRT1 and SIRT3 deacetylate AceCS1 and AceCS2, respectively, promoting their activity [18]. Both SIRT1 and SIRT3 play an important role during energy-poor diets [19]. In particular, under long-term fasting or CR, acetate is released from the liver and utilized for energy production in extraepatic tissues following AceCS2 activation [16,20]. In this context, SIRT3 might modulate the reprogramming of mitochondria to low energy input [21]. The SIRT1/3-dependent regulation of AceCS1/2 and the implication of the two Sirtuins in aging and in the CR-mediated longevity response [13,22,23], have suggested an involvement of the acetate metabolism in the aging process [16]. Similarly to SIRT1/3, a Sir2 ortholog, CobB, in *Salmonella enterica* activates through deacetylation the acetyl-CoA synthetase (Acs in bacteria and yeast) allowing acetate utilization for acetyl-CoA synthesis and bacterial growth on acetate [17,24]. In *S.cerevisiae* two Acs isoenzymes, Acs1 and Acs2, are present which differ with respect to kinetic properties and cellular localization [25,26]. To date, there is no evidence of a reversible acetylation involved in their enzymatic activation [25]. Interestingly, Acs2 is required for replicative longevity [25], further supporting the notion that the acetate metabolism can play an important role during aging. This is also suggested by data showing that genetic interventions which drive yeast metabolism away from acetic acid production increase CLS [11].

In this study, we provide evidence that in the budding yeast, *SIR2* inactivation actually influences positively the acetate utilization by way of an increased flux of the glyoxylate/gluconeogenic pathway. In the chronological aging paradigm, this implies low levels of toxic extracellular factors (ethanol and acetic acid) and an increase of protective intracellular factors (trehalose) in the *sir2Δ* cultures which all together may favor a better long-term survival and extension of CLS.

2. Materials and methods

2.1. Yeast strains and growth conditions

All yeast strains used in this work are listed in Table S1. All deletion strains were generated by PCR-based methods [27]. Genomically 3HA-tagged strains were obtained as described [28]. The tagged strains were undistinguishable from the congenic untagged ones with respect to overall morphology, cellular volumes, duplication times and CLS. The accuracy of all gene replacements and correct deletions/integrations was verified by PCR with flanking and internal primers. Primer sequences are available upon request. Standard methods were used for DNA manipulation and yeast transformation. Yeast cells were grown in batches at 30 °C in rich medium (YEP, 1% w/v yeast extract, 2% w/v bacto peptone) with the indicated carbon source at 2%. For the acetate-YEP medium (pH 4 or 5.8) precalculated amounts of 0.2 M acetic acid and 0.2 M sodium acetate solutions were mixed and added to YEP medium to obtain the required pH and molarity (0.1 M). pH 5.8 was selected since it was the initial pH of the unbuffered YEP medium. For cells grown in minimal medium (Difco Yeast Nitrogen Base without amino acids, 6.7 g/l), auxotrophies were compensated for with a four-fold excess of supplements [12]. All strains were inoculated at the same cellular density (culture volume no more than 20% of the flask volume). Growth was monitored by determining cell number using a Coulter Counter-Particle Count and Size Analyzer, as described [29]. Doubling time (Td) was obtained by linear regression of the cell number increase over time on a semilogarithmic plot.

2.2. Ethanol and acetate pulses

Yeast cells were grown in glucose-limited chemostat cultures [30] at a dilution rate of 0.15 h^{-1} and with an airflow of 0.8 l/min. Mineral medium was prepared according to [31], supplemented with glucose at 7 g/l. The pH was kept constant at 4.5 by the automatic addition of 2 M KOH. Once chemostat cultures achieved the steady-state, the medium feed and the effluent pumps were switched off. At this time-point, a concentrated solution of ethanol or sodium acetate (pH 4.5) was injected aseptically giving an initial concentration in the chemostat of about 90 mM of ethanol and 3.3 mM of acetate. Samples were collected at different time-points for analyses of metabolite contents. Cell dry weight was determined as described [32]. Off-gas analysis (O_2 and CO_2) was performed with a BM2001 gas analyzer (Bioindustrie Mantovane, Italy). O_2 consumption and CO_2 production were calculated as in [33]. Each pulse experiment was carried out in triplicate. Trends reported refer to a representative experiment.

2.3. Metabolite measurements

At designated time-points, aliquots of the yeast cultures were centrifuged and both pellets (washed twice) and supernatants were frozen at −20 °C until used. Glucose, ethanol and acetate concentrations in the growth medium were determined using enzymatic assays (K-HKGLU, K-ETOH and K-ACET kits from Megazyme). Intracellular trehalose was extracted and measured as described [34]. After incubation with trehalase (Sigma), the amount of glucose generated from trehalose hydrolysis was determined using the K-HKGLU kit. The pre-existent glucose in each sample was measured in a parallel reaction without trehalase and subtracted from the total glucose. Total protein concentration was estimated using the BCA™ Protein Assay Kit (Pierce).

Final values represent the average of three independent experiments. Differences in measurements were assessed by Student's *t*-test. The level of statistical significance was set at a P value of ≤ 0.05.

2.4. Enzyme assays

Cell extracts were prepared from harvested cells as described [35] except that cells were broken with acid-washed glass beads by shaking on a vortex for several cycles interspersed with cooling on ice. Immediately after preparation of cell-free extracts, Pck1 and Icl1 activities were determined [35].

2.5. Immunoprecipitation and Western analysis

Cellular extracts for anti-HA immunoprecipitation were prepared essentially as described [36] in the presence of protease inhibitors (1 mM phenylmethanesulfonyl fluoride and Complete EDTA-free Protease Inhibitor Cocktail Tablets, Roche) and histone deacetylase inhibitors (100 μM Trichostatin A, 50 mM nicotinamide and 50 mM sodium butyrate). A crude lysate aliquot was stored at −20 °C as immunoprecipitation input control. For immunoprecipitation, lysates (about 500 μg) were incubated with 2 μg of anti-HA mAb (12CA5; Roche) at 4 °C overnight, followed by the addition of 50 μl Dynabeads Protein A (Dynal Biotech) for 2 h. After five washes with washing buffer (50 mM Tris, pH 7.4, and 50 mM NaCl) at 4 °C, bound proteins were eluted by boiling in SDS sample buffer, resolved by SDS-PAGE and then subjected to Western analysis. Primary antibodies used were: anti-HA mAb (12CA5; Roche), anti-acetylated-lysine mAb (Ac-K-103; Cell Signaling) and anti-3-phosphoglycerate kinase (Pgk1) mAb (22C5; Invitrogen). Secondary antibodies were purchased from Amersham. Binding was visualized with the ECL Western Blotting Detection Reagent (Amersham). Afterwards ECL detection, films were scanned on a Bio-Rad GS-800 calibrated imaging densitometer and quantified with Scion Image software.

2.6. Acetic acid sensitivity

Exponentially growing cells on glucose were harvested and resuspended (10^7 cells/ml) in YEP/glucose (YEPD) pH 5.8, YEPD pH 4 or YEPD pH 3 (set with HCl) medium containing 80, 100 or 120 mM acetic acid. Cells were incubated for 200 min at 30 °C with shaking [37]. After treatment, cells (serially diluted) were spotted onto YEPD plates. Plates were incubated at 30 °C for 3 days.

2.7. CLS determination

Survival experiments in expired medium were performed on cells grown either in YEPD or in minimal medium (with a four-fold excess of supplements)/2% glucose as described by [12,38]. During growth, cell number and extracellular glucose, ethanol and acetic acid were measured in order to define the growth profile (exponential phase, diauxic shift, post-diauxic phase and stationary phase) of the culture. Cell survival was monitored by harvesting aliquots of cells starting 72 h (Day 3, first age-point) after the diauxic shift (Day 0). CLS was measured according to [12] by counting colony-forming units (CFUs) every 2–3 days. The number of CFUs on Day 3 was considered the initial survival (100%).

Survival experiments in water and in water containing ethanol were performed on cells grown in minimal medium/glucose (with a four-fold excess of supplements) as described by [12]. Every 48 h, ethanol was added to the culture after washing at a concentration (6 g/l) equal to that found in the expired medium at Day 0. In parallel, 50 mM pyrazole (Sigma) was added [39]. Viability was measured as described above.

For CLS determination in media-swap experiments, cells were grown in minimal medium/glucose (with a four-fold excess of supplements) and at Day 1 after the diauxic shift harvested by centrifugation. Cell pellets were washed and then resuspended in the filtered original medium or equivalently conditioned one of the indicated strain.

3. Results and discussion

3.1. Chronological aging sir2Δ cells avoid extracellular acetic acid accumulation

In chronological aging, two by-products of glucose fermentation, ethanol and acetic acid, which accumulate in the yeast culture medium, have CLS-shortening effects [11,12]. Since CLS extension in *sir2Δ* mutants is associated with an increase in the depletion of extracellular ethanol, which is re-introduced into the metabolism *via* its oxidation to acetate (Fig. 1A), we wondered whether the extracellular acetate/acetic acid (see below) was also influenced by *SIR2* inactivation. To this end, we analyzed the kinetics of ethanol and acetate accumulation in wild type (wt) and *sir2Δ* cultures during growth on YEP/2% glucose (YEPD) and the subsequent utilization of these C2 substrates during the post-diauxic phase. During the exponential phase, when growth is sustained by a prevalent fermentative metabolism, the glucose decrease was accompanied by ethanol accumulation that in both strains followed the same kinetics (Fig. 1B). After the diauxic shift, when cells switched to a respiration-based metabolism, ethanol was depleted more rapidly in the *sir2Δ* culture compared with the wt one (Fig. 1B and C). With regard to acetate, in the wt culture, its concentration initially increased and then slowed down (Fig. 1D). Interestingly, in the *sir2Δ* culture very low levels of excreted acetate were detected (Fig. 1D). Moreover, measurements of ethanol and acetate in the culture media of cells grown in minimal medium also revealed that, after the diauxic shift, in the *sir2Δ* culture, ethanol was exhausted earlier than in the wt one (Fig. S1A) in line with changes observed by [12] and acetate was detected at very low levels (Fig. S1B). Thus, lack of Sir2 affects the extracellular abundance of two chronological aging factors, ethanol and acetic acid, but unlike the case with ethanol, the reduced accumulation of acetic acid seems to be linked to a reduced secretion of the fermentation product.

It is known that culturing cells in rich YEPD medium rather than in synthetic defined minimal medium extends CLS [40–42] and this was the case for both wt and *sir2Δ* cultures (Fig. 1E and F). Besides, *sir2Δ* cells aged in YEPD medium lived longer than the wt ones (Fig. 1E). In agreement with [12], no significant difference in CLS was observed between the two strains grown on minimal medium when CFUs were monitored until 99.9% of the population died (Fig. 1F). However, CFUs monitored below this value (Fig. 1F) and some experiments performed in another genetic background [12] may suggest that *SIR2* inactivation also affects positively chronological survivability in minimal medium. Known interventions that increase CLS, such as CR, promote longevity by reducing also the extracellular amount of acetic acid [11,43]. It is therefore conceivable that the low level of this compound in the *sir2Δ* medium might contribute to determine the *sir2Δ* long-lived phenotype.

In parallel, since ethanol and acetate can be utilized by *S.cerevisiae* as sole carbon and energy source under aerobic conditions, we also examined the growth behavior of the *sir2Δ* mutant during exponential growth on these nonfermentable substrates. A marked decrease in the Td of the *sir2Δ* mutant was detected for cells growing on YEP/ethanol compared with the wt, while for cells grown on glucose no significant differences were observed (Table 1). Similar results were obtained for YNB-based medium (data not shown). Given that ethanol enters the cells by passive diffusion, a faster growth can be indicative of a faster ethanol catabolism in agreement with the faster depletion of ethanol in the *sir2Δ* culture reported in Fig. 1, Fig. S1 and by [12]. When cells were grown on acetate, pH 5.8, the Td of the wt and of the *sir2Δ* strain was similar. Nevertheless, lowering the pH to 4 favored the mutant strain growth with respect to the wt that displayed a severe growth defect (Fig. S2A). Uptake of acetate is linked to a proton symport mechanism accompanied by passive diffusion of the undissociated acid [44,45]. The acetic/acetate couple forms a buffer system: at pH 4, acetic acid (pKa 4.75) is substantially undissociated while at pH 5.8 the amount of the charged acetate anion considerably increases. Consequently, at pH 4 the uptake of acetate is facilitated because passive diffusion is elevated. Once inside the cell (pH close to neutral), acetic acid dissociates causing intracellular acidification that, in turn, is thought to have negative effects on yeast metabolic activity explaining why acetate is generally toxic at pH 4 [37,45]. The fact that the *sir2Δ* strain grows on acetate at pH 4 also suggests an increased resistance of these cells to acetic acid. Consistently, *sir2Δ* cells showed less sensitivity to acetic acid stress at low pH (Fig. S2B).

3.2. Lack of Sir2 correlates with a more efficient acetate utilization

In order to better define the metabolic consequences of the *SIR2* inactivation and to obtain reliable quantitative measurements of metabolite productions, we carried out experiments in chemostat. A prototrophic *sir2Δ* strain was generated in a GRF18 background (Table S1) since auxotrophic strains are less suited for quantitative physiological analyses [46]. In this genetic background, the effects of *SIR2* inactivation were similar to those reported in Fig. 1 and Table 1 (data not shown). Aerobic glucose-limited chemostat cultures at a low dilution rate (0.15 h^{-1}) were set up for prototrophic *sir2Δ* and wt strains. In both cultures the high biomass yield, the absence of fermentation products and CO_2 production (biomass and CO_2 were the only products), all indicated that the metabolism was fully respiratory (data not shown) [30]. To this starting condition, where the catabolite repression is alleviated and the enzymes for catabolism of C2 compounds are partially derepressed [47], an ethanol pulse was applied with the simultaneous switch-off of the glucose influx/efflux. In such a way, cells grow using ethanol as the sole carbon source. As shown in Fig. 2A and Table 2, the ethanol specific consumption rate (qEtOH,

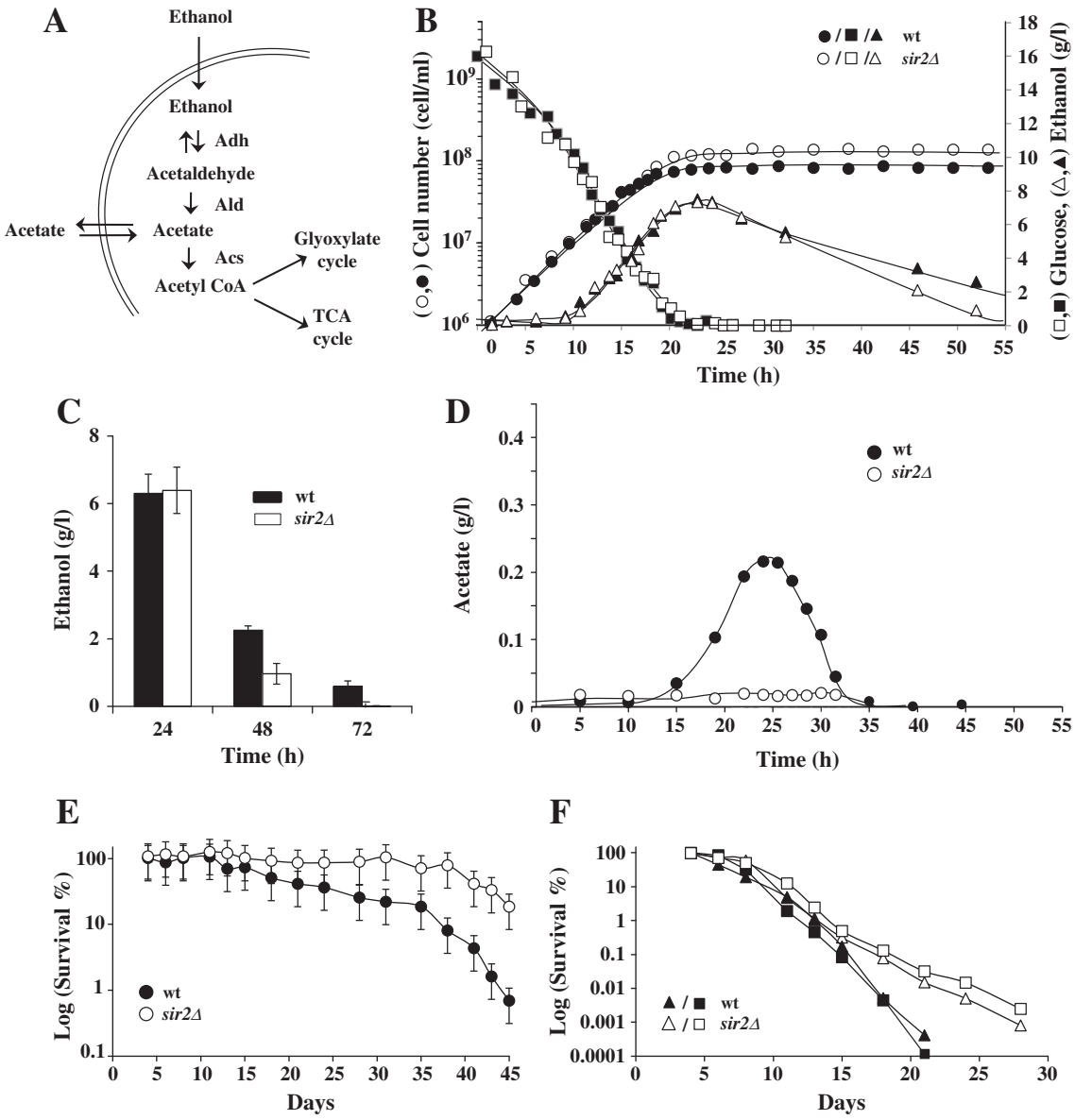

Fig. 1. *SIR2* inactivation affects the extracellular abundance of ethanol and acetate produced by glucose fermentation. (A) Scheme of the metabolic steps allowing ethanol utilization. Adh: alcohol dehydrogenase; Ald: aldehyde dehydrogenase; Acs: acetyl-CoA synthase. (B) Wild type (wt) and *sir2*Δ cells were grown in YEP/2% glucose (YEPD) and cell growth was monitored by counting cell number over time. Extracellular concentrations of ethanol and glucose (B) and acetate (D) were also measured in medium samples collected at different time-points. One representative experiment is shown. (C) Bar charts of ethanol concentrations measured in the media of cultures described in (B). Data were obtained from mean values determined in three independent experiments. Standard deviations are indicated. (E) CLS of wt and *sir2*Δ mutant cells grown on YEPD. At every time-point, viability was determined by counting CFUs on YEPD plates. 72 h after the diauxic shift (Day 3), was considered the first age-point (see Materials and methods). Error bars are the standard deviation of three replicates. (F) CLS of wt and *sir2*Δ mutant cells grown on minimal medium/2% glucose (with a four-fold excess of supplements). At every time-point, viability was measured as in (E). Two representative experiments are shown.

Table 1
*sir2*Δ mutant growth is favored on ethanol.

Medium	Strain	Td (h)*
Glucose	wt	1.39 ± 0.09
	*sir2*Δ	1.41 ± 0.03
Ethanol	wt	4.38 ± 0.36
	*sir2*Δ	3.30 ± 0.24
Acetate pH 5.8	wt	2.19 ± 0.2
	*sir2*Δ	2.21 ± 0.15

Duplication time (Td) of the indicated strains growing on different carbon sources. *Td was calculated as ln2/k, where k is the constant rate of exponential growth. Data represent the average of three independent experiments. Standard deviations are indicated.

mmol g^{-1} DW h^{-1}) for the *sir2*Δ strain was higher than the wt one indicating that *SIR2* inactivation accelerates ethanol catabolism. Moreover, following the ethanol pulse, an immediate secretion of acetate was observed in both cultures (Fig. 2B) implying an increased metabolic flux through acetaldehyde dehydrogenase towards acetate (Fig. 1A) in line with other ethanol pulse experiments [48,49]. Acetate accumulation in the medium is due to an imbalance between its production rate from acetaldehyde and its conversion rate into acetyl-CoA (Fig. 1A). Interestingly, the *sir2*Δ strain not only secreted less acetate than the wt, but after a transient accumulation, the concentration of acetate started to decrease quickly despite high levels of ethanol in the medium (Fig. 2A and B). After 2 h from the pulse in the mutant, ethanol and acetate were consumed in parallel (ethanol–acetate cometabolism) and in the medium the latter was exhausted first (Fig. 2A and B). This indicates that in the *sir2*Δ strain, acetate is metabolized faster than it

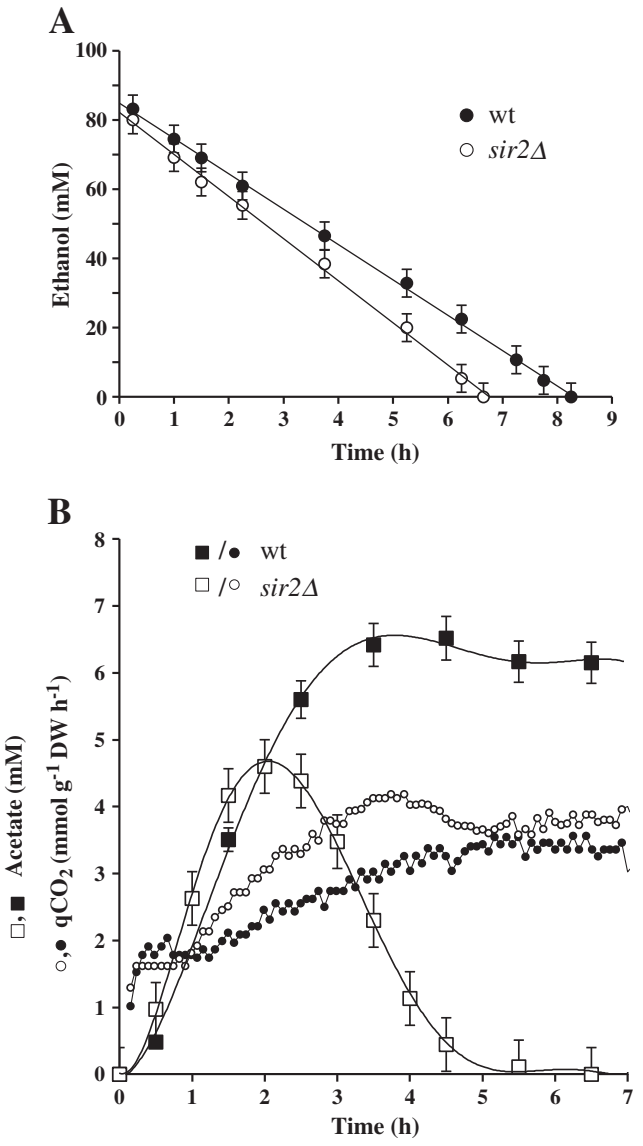

Fig. 2. *SIR2* inactivation affects acetate metabolism. Wild type (wt) and *sir2*Δ cells were grown in glucose-limited chemostat cultures (0.15 h^{-1} dilution rate) and at the steady-state (time 0) an ethanol pulse was applied (about 90 mM final concentration). Extracellular ethanol (A) and acetate (B) were measured in the medium at different time-points after ethanol addition. Standard deviations are indicated. In parallel, the concentration of carbon dioxide in the off-gas was monitored. qCO_2: carbon dioxide specific production rate. Data are reported as a function of the time after ethanol addition.

is produced implying an increased metabolic flux downstream from the acetate. Indeed, when an acetate pulse was applied to the aerobic glucose-limited chemostat cultures set up for the *sir2Δ* and wt strains, the acetate specific consumption rate (qAc, mmol g^{-1} DW h^{-1}) of the *sir2Δ* strain was higher than the wt one (Table 2) supporting the assumption of a more efficient acetate metabolism in the mutant.

Table 2
SIR2 inactivation increases ethanol and acetate specific consumption rates.

	Strain	
	wt	*sir2Δ*
qEtOH (mmol g^{-1} DW h^{-1})	2.56 ± 0.08	4.24 ± 0.05
qAc (mmol g^{-1} DW h^{-1})	0.65 ± 0.04	0.79 ± 0.03

Ethanol (qEtOH) and acetate (qAc) specific consumption rates were determined in ethanol and acetate pulse experiments, respectively. Data represent the average ± standard deviation of three independent replicates.

Acetate metabolism requires acetate activation by acetyl-CoA synthetase isoenzymes Acs1 and Acs2, to acetyl-CoA which can be used to fuel the glyoxylate and TCA cycles. In addition, acetyl-CoA is used for synthesis of macromolecules which requires active gluconeogenesis [50]. It has been reported that increase in Acs activity did not result in enhanced acetate utilization [51,52] indicating that reactions downstream from Acs mainly control the *in vivo* rate of acetate activation. In this context, off-gas analyses during the ethanol pulse gave some information about the reactions downstream from acetyl-CoA that were influenced by *SIR2* inactivation. No significant difference in the oxygen specific consumption rate (qO_2, mmol g^{-1} DW h^{-1}) between the wt and the *sir2Δ* strains was found (Fig. S3). This is indicative of a similar mitochondrial respiratory activity. On the contrary, a higher CO_2 production rate was measured in the mutant during acetate accumulation and utilization (Fig. 2B) suggesting that decarboxylation/s along the pathway of the acetate metabolism is/are increased.

3.3. Lack of Sir2 correlates with enhanced gluconeogenesis

Phosphoenolpyruvate carboxykinase (Pck1) catalyzes the rate-limiting step in gluconeogenesis by converting a C4 compound such as oxaloacetate (OAA) to a C3, phosphoenolpyruvate. Pck1 is subjected to different layers of regulation including posttranslational acetylation at K514 by Esa1 which is crucial for its enzymatic activity, for the ability of yeast cells to grow on nonfermentable carbon sources and for CLS extension under a severe form of CR such as water starvation. Interestingly, Sir2 is the enzyme responsible for Pck1 deacetylation [53]. In the *sir2Δ* strain, during the ethanol pulse and during the growth in batch on ethanol, Pck1 enzymatic activity was higher than that of the wt (Fig. 3A and B). In addition, chronological aging *sir2Δ* cells had higher levels of Pck1 enzymatic activity compared with the wt (Fig. 3C and D). Since *SIR2* loss of function increases acetylated Pck1 [53], these results prompted us to investigate whether the increase of Pck1 enzymatic activity detected in the *sir2Δ* cells was associated with an increase of the acetylated form of the enzyme. To this end, wt and *sir2Δ* strains expressing a 3HA-tagged version of the endogenous Pck1 were generated. As shown in Fig. 3D and E and S4, *SIR2* deletion did not affect Pck1-3HA levels, while the amount of acetylated Pck1-3HA increased in the *sir2Δ* strain compared with the wt. This suggests that *SIR2* deletion correlates with an *in vivo* increase of the acetylated enzymatic active Pck1 which, in turn, may favor the gluconeogenic flux.

During growth on C2 compounds, the glyoxylate cycle is generally assumed to be the exclusive source of OAA (derived from two molecules of acetyl-CoA) which enters the gluconeogenic pathway [50]. Measurements of the enzymatic activity of isocitrate lyase (Icl1), which is one of the unique enzymes of the glyoxylate cycle, showed higher levels in the *sir2Δ* mutant compared with the wt during both the ethanol pulse and batch growth (Fig. 4A). This further supports the notion of an increased assimilation of C2 units by the way of the glyoxylate/gluconeogenic pathway linked to *SIR2* inactivation and also gives some experimental evidence of the model proposed by [53] concerning the role played by the Pck1 acetylation state in the control of the gluconeogenic flux.

Gluconeogenesis switches the direction of metabolite flow towards the essential biosynthetic precursor, glucose-6-phosphate, which is also needed for glycogen and trehalose stores. In particular, trehalose has been proposed to be a key determinant of the quiescent metabolic state as a fuel reserve that enables yeast to survive starvation and then rapidly proliferate upon return to favorable growth conditions [54]. During stationary phase, in both the wt and *sir2Δ* strains the trehalose content increased but in the mutant this disaccharide is more abundant (Fig. 4B), in line with transcriptional data showing down-regulation of genes involved in utilization/breakdown of trehalose [12]. Enhanced intracellular trehalose levels might contribute to the reported stress-resistant phenotype of the mutant [12] and to improve its survivability and CLS.

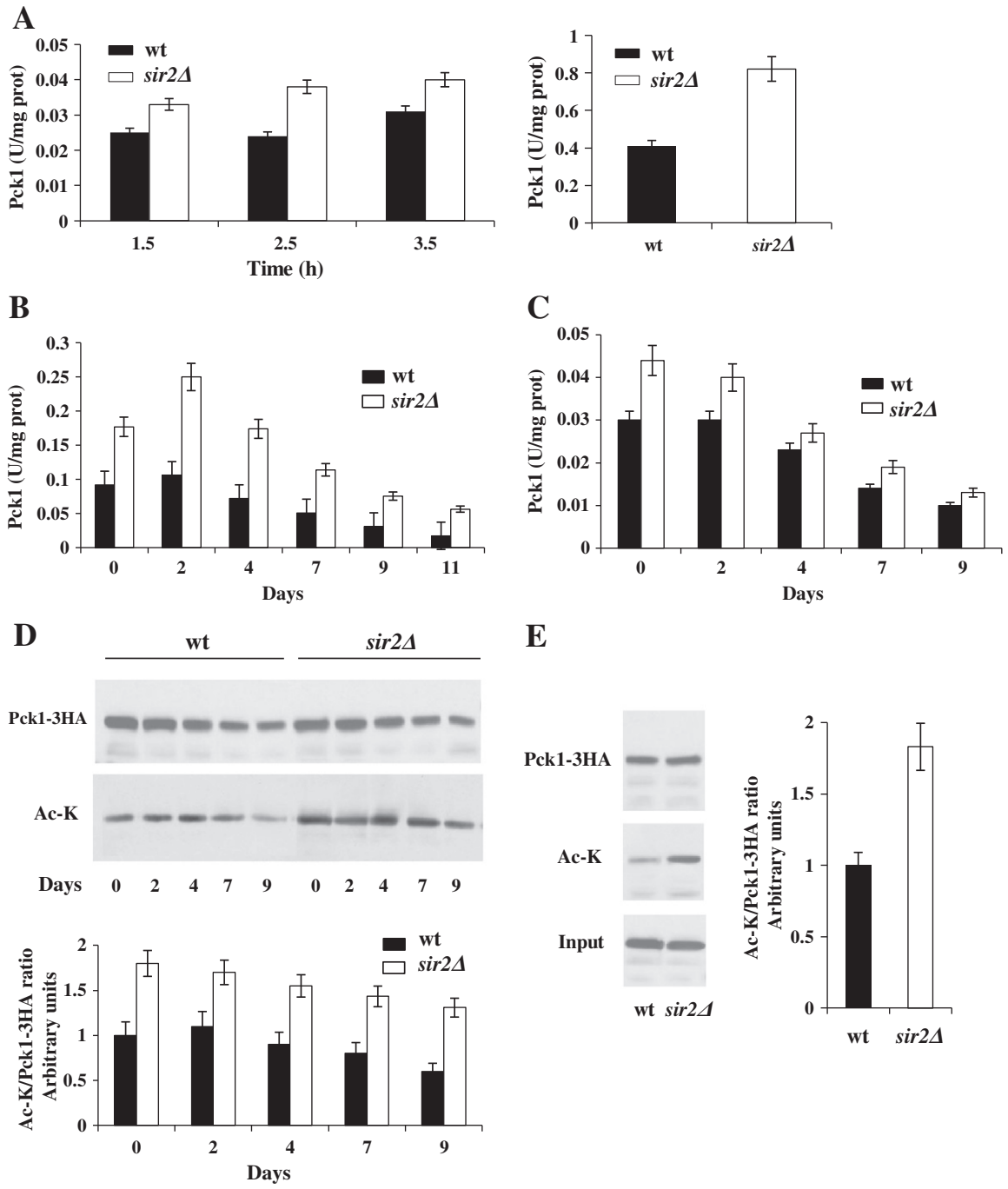

Fig. 3. *SIR2* inactivation increases acetylated Pck1 in concert with increased enzymatic activity. (A) Pck1 enzymatic activity was measured at the indicated time-points after the ethanol addition to glucose-limited chemostat cultures of Fig. 2 (left panel) and in wt and *sir2*Δ cells exponentially growing on ethanol in batch (right panel). Pck1 enzymatic activity was also measured at the indicated time-points during chronological aging in YEPD (B) and minimal medium/2% glucose (C). Day 0, diauxic shift. Error bars are the standard deviation of three replicates. (D) Wt and *sir2Δ* cells expressing 3HA-tagged Pck1 were grown in minimal medium. During chronological aging at the indicated time-points total extracts (shown in Fig. S4) were collected, immunoprecipitated with anti-HA antibody and subjected to Western analysis. Immunodecoration was performed with anti-HA and anti-Ac-K antibodies. Representative blots are shown. For each lane, band intensities were quantified by densitometry and the ratio of Ac-K to Pck1-3HA was plotted (lower panel). Standard deviations are indicated ($P \leq 0.01$). Day 0, diauxic shift. (E) Total extracts collected from wt and *sir2Δ* cells expressing 3HA-tagged Pck1, exponentially growing on ethanol were immunoprecipitated with anti-HA antibody and subjected to Western analysis. Immunodecoration was performed with anti-HA and anti Ac-K antibodies. Input, total protein extracts probed with anti-HA antibody. Band intensities were quantified as in (D) and the ratio Ac-K/Pck1-HA plotted (left panel). Standard deviations are indicated ($P \leq 0.01$).

Fig. 4. *SIR2* inactivation increases acetyl-CoA flux towards glyoxylate-requiring gluconeogenesis. (A) Icl1 enzymatic activity was measured at the indicated time-points after the ethanol addition to glucose-limited chemostat cultures of Fig. 2 (left panel) and in wt and *sir2*Δ cells exponentially growing on ethanol in batch (right panel). (B) Intracellular trehalose content of the indicated strains grown as described in Fig. 1B. Measurements were performed during the exponential phase (EXP) up to the stationary one. Histograms were obtained from mean values determined in three independent experiments. Standard deviations are indicated. (C) CLS of the indicated strains grown on minimal medium. One representative experiment is shown. In parallel, extracellular concentrations of ethanol (D) and acetate (E) were measured in medium samples collected at different time-points. Day 0, diauxic shift. Data were obtained from mean values determined in three independent experiments. Standard deviations are indicated. (F and G) CLS of wt, *icl1Δ* and *sir2Δ* mutant cells grown as in (C) which have been harvested and resuspended in their cell free original media or subjected to cell free media-swap at Day 1 after the diauxic shift. One representative experiment is shown.

Starting from the aforementioned results, we analyzed the effects on CLS and on extracellular ethanol and acetate levels following *PCK1* or *ICL1* deletions in the *sir2Δ* background. As depicted in Fig. 4C, loss of *PCK1* significantly reduced CLS in agreement with [53] but interestingly this was also the case for *ICL1* deletion, further underlying a connection between gluconeogenesis and chronological longevity.

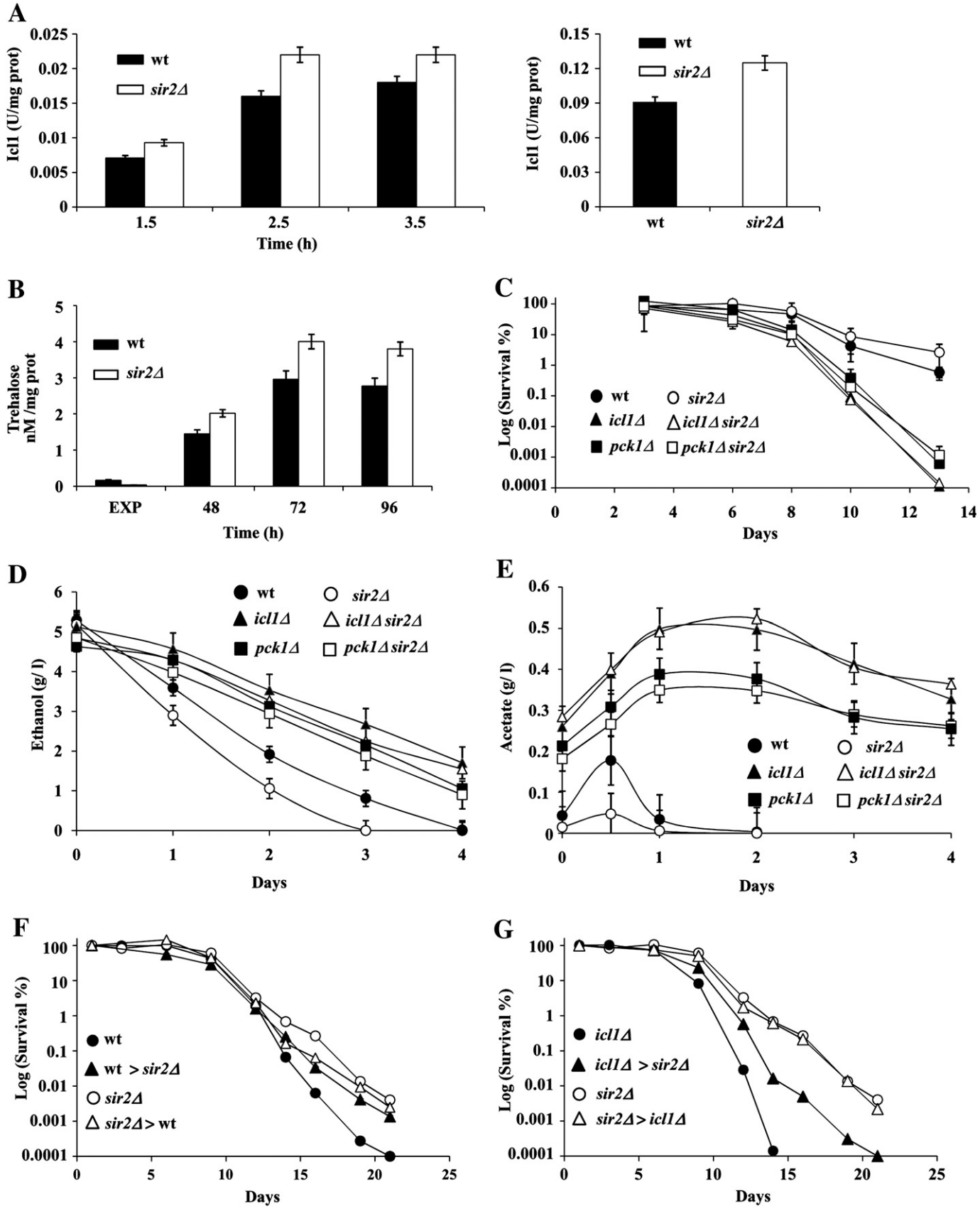

Moreover, *SIR2* deletion did not influence the CLS of *pck1Δ* mutants and did not influence the CLS of *icl1Δ* mutants either (Fig. 4C). Concerning extracellular ethanol and acetate, the effect produced by both the single *PCK1* and *ICL1* deletions was opposite of that elicited by *SIR2* deletion. In fact, in both single *pck1Δ* and *icl1Δ* cultures, ethanol was exhausted later than in the wt one (Fig. 4D) and acetate was detected at higher levels (Fig. 4E). In addition, *pck1Δ* and *icl1Δ* cells showed more sensitivity to acetic acid stress at low pH (Fig. S5). Similar to the effect on CLS, *PCK1* and *ICL1* were epistatic to *SIR2* in the pathway involved in the metabolism of ethanol and acetate, since *SIR2* deletion did not affect either ethanol consumption (Fig. 4D), acetate levels (Fig. 4E) or acetic acid sensitivity (Fig. S5) that were detected in the *pck1Δ* and *icl1Δ* mutants. We next performed a media-swap experiment among wt, *icl1Δ* and *sir2Δ* cultures. The three strains were grown on minimal medium and, at Day 1 after the diauxic shift, cultures were centrifuged and media were exchanged. The media exchange did not influence the chronological survival of the *sir2Δ* strain (Fig. 4F and G) whose CLS was the same despite more ethanol and acetate present in the *icl1Δ* pre-conditioned medium, (Fig. 4D and E). On the contrary, the *sir2Δ* pre-conditioned medium had a beneficial effect on the CLS of both wt and *icl1Δ* strains (Fig. 4F and G). Interestingly, resuspension of *icl1Δ* cells in the *sir2Δ* pre-conditioned medium increased their CLS to the same extent as that of the wt maintained in its original medium (Fig. 4F and G). These results further show that the *SIR2* deletion not only decreases the level of extracellular factors which contribute negatively to CLS, but also enables the cells to better cope with them. With regard to acetic acid, its role during CLS, it is a matter of debate and a clear consensus has not been reached yet [55]. Although preventing acidification of the culture media which is mainly due to acetic acid is sufficient to extend CLS [11,42], it is unlikely that the physiological extracellular accumulation of acetic acid during CLS standard experiments may be the toxic determinant in itself.

To sum up, collectively these data indicate that a lack of Sir2 deacetylase activity positively affects acetate metabolism by enhancing the glyoxylate-requiring gluconeogenesis. This also has a stimulatory effect on ethanol catabolism in order to support the more rapid metabolic flux downstream from the acetate activation into acetyl-CoA. It follows that i) *sir2Δ* cells grow better than the wt on ethanol and acetate and ii) in the post-diauxic phase, following glucose exhaustion, these cells avoid acetate accumulation in the medium and deplete extracellular ethanol faster. This C2 compound indirectly has CLS-shortening effects by being metabolized to acetate. In fact, it has been previously reported that the addition of ethanol to water can prevent CLS extension of chronologically aging cells associated with their transfer to water [12]. This is a severe form of CR which dramatically extends CLS and such a salutary effect is more pronounced in cells lacking Sir2 [12 and Fig. 5]. In line with this, ethanol add-back wt and *sir2Δ* cultures had a reduced CLS compared with cells incubated in water alone (Fig. 5). Moreover, inhibition of ethanol oxidation to acetate by pyrazole, an inhibitor of alcohol dehydrogenase 2 [39], abrogated the pro-aging signaling seen with ethanol producing a CLS extension similar to that observed in water (Fig. 5).

Enhancement in the intracellular flux of the central metabolic pathways such as glycolysis/gluconeogenesis, can be rarely ascribed to changes in a single enzyme since flux control is shared by multiple steps and not usually localized in only one step. Nevertheless, a particular enzymatic reaction can exert a high degree of control over the flux along a pathway and, hence, strongly influence the rate of the flux itself. Thus, except for enzymes subjected to allosteric regulation or feedback inhibition, it is reasonable to speculate that if the rate of this crucial step could be increased, the overall pathway flux might also increase. In this context, probably the major signal which triggered the metabolic changes leading to an improved assimilation of C2 units by the glyoxylate-requiring gluconeogenesis in the *sir2Δ* mutant is the increase in the main flux-controlling step of the gluconeogenesis, namely the Pck1 enzymatic activity. This increase can be brought about by the increase in the acetylated active form of Pck1 due to the lack of the Sir2-targeted deacetylation. Furthermore, the enhancement in the direction of metabolite flow towards glucose-6-phosphate in the *sir2Δ* may not only reduce pro-aging extracellular signaling from ethanol/acetic acid but also increase the accumulation of trehalose creating a beneficial environment that is important for the long-term survival of non-dividing cells.

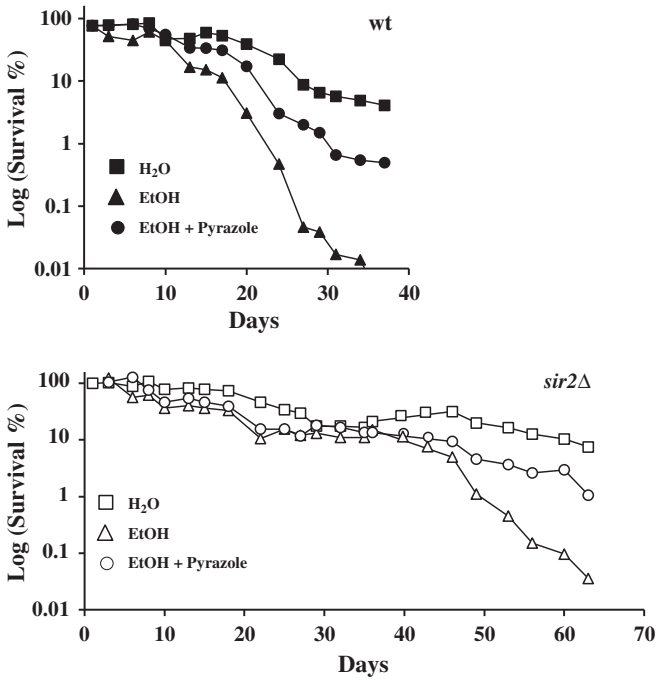

Fig. 5. Pyrazole suppresses the CLS-shortening effect of ethanol. Wt and *sir2Δ* cells grown in minimal medium were switched to water, water/ethanol (6 g/l) or water/ethanol/pyrazole (50 mM) at Day 1. Every 48 h, cultures were resuspended in fresh water and each time, ethanol and pyrazole were added when indicated. At every time-point, viability was measured by counting CFUs on YEPD plates. Survival of cells in their exhausted medium was also monitored as control (reported in Fig. 1F). One representative experiment is shown.

Supplementary data to this article can be found online at http://dx.doi.org/10.1016/j.bbamcr.2012.11.008.

Acknowledgements

The authors are grateful to Neil Campbell for the English revision. This work was supported by FAR 2010 to M.V.

References

[1] C.J. Kenyon, The genetics of ageing, Nature 464 (2010) 504–512.
[2] N. Kourtis, N. Tavernarakis, Cellular stress response pathways and ageing: intricate molecular relationships, EMBO J. 30 (2010) 2520–2531.
[3] K.A. Steinkraus, M. Kaeberlein, B.K. Kennedy, Replicative aging in yeast: the means to the end, Annu. Rev. Cell Dev. Biol. 24 (2008) 29–54.
[4] P. Fabrizio, V.D. Longo, The chronological life span of *Saccharomyces cerevisiae*, Aging Cell 2 (2003) 73–81.
[5] B. Smets, R. Ghillebert, P. De Snijder, M. Binda, E. Swinnen, C. De Virgilio, J. Winderickx, Life in the midst of scarcity: adaptations to nutrient availability in *Saccharomyces cerevisiae*, Curr. Genet. 56 (2010) 1–32.
[6] L. Fontana, L. Partridge, V.D. Longo, Extending healthy life span: from yeast to humans, Science 328 (2010) 321–326.
[7] M. Kaeberlein, Lessons on longevity from budding yeast, Nature 464 (2010) 513–519.
[8] W. Mair, A. Dillin, Aging and survival: the genetics of life span extension by dietary restriction, Annu. Rev. Biochem. 77 (2008) 727–754.
[9] M. Wei, P. Fabrizio, J. Hu, H. Ge, C. Cheng, L. Li, V.D. Longo, Life span extension by calorie restriction depends on Rim15 and transcription factors downstream of Ras/PKA, Tor, and Sch9, PLoS Genet. 4 (2008) e13.
[10] Y. Pan, Mitochondria, reactive oxygen species, and chronological aging: a message from yeast, Exp. Gerontol. 46 (2011) 847–852.

[11] C.R. Burtner, C.J. Murakami, B.K. Kennedy, M. Kaeberlein, A molecular mechanism of chronological aging in yeast, Cell Cycle 8 (2009) 1256–1270.
[12] P. Fabrizio, C. Gattazzo, L. Battistella, M. Wei, C. Cheng, K. McGrew, V.D. Longo, Sir2 blocks extreme life-span extension, Cell 123 (2005) 655–667.
[13] S. Imai, L. Guarente, Ten years of NAD-dependent SIR2 family deacetylases: implications for metabolic diseases, Trends Pharmacol. Sci. 31 (2010) 212–220.
[14] E.L. Bell, L. Guarente, The SirT3 divining rod points to oxidative stress, Mol. Cell 42 (2011) 561–568.
[15] M.C. Haigis, D.A. Sinclair, Mammalian sirtuins: biological insights and disease relevance, Annu. Rev. Pathol. 5 (2010) 253–295.
[16] T. Shimazu, M.D. Hirschey, J.Y. Huang, L.T. Ho, E. Verdin, Acetate metabolism and aging: an emerging connection, Mech. Ageing Dev. 131 (2010) 511–516.
[17] A.J. Wolfe, The acetate switch, Microbiol. Mol. Biol. Rev. 69 (2005) 12–50.
[18] W.C. Hallows, S. Lee, J.M. Denu, Sirtuins deacetylate and activate mammalian acetyl-CoA synthetases, Proc. Natl. Acad. Sci. U. S. A. 103 (2006) 10230–10235.
[19] L. Guarente, The logic linking protein acetylation and metabolism, Cell Metab. 14 (2011) 151–153.
[20] X. Qiu, K.V. Brown, Y. Moran, D. Chen, Sirtuin regulation in calorie restriction, Biochim. Biophys. Acta 1804 (2010) 1576–1583.
[21] W.C. Hallows, W. Yu, B.C. Smith, M.K. Devries, J.J. Ellinger, S. Someya, M.R. Shortreed, T. Prolla, J.L. Markley, L.M. Smith, S. Zhao, K.L. Guan, J.M. Denu, Sirt3 promotes the urea cycle and fatty acid oxidation during dietary restriction, Mol. Cell 41 (2011) 139–149.
[22] S. Someya, W. Yu, W.C. Hallows, J. Xu, J.M. Vann, C. Leeuwenburgh, M. Tanokura, J.M. Denu, T.A. Prolla, Sirt3 mediates reduction of oxidative damage and prevention of age-related hearing loss under caloric restriction, Cell 143 (2010) 802–812.
[23] L. Zhong, R. Mostoslavsky, Fine tuning our cellular factories: sirtuins in mitochondrial biology, Cell Metab. 13 (2011) 621–626.
[24] V.J. Starai, H. Takahashi, J.D. Boeke, J.C. Escalante-Semerena, Short-chain fatty acid activation by acyl-coenzyme A synthetases requires SIR2 protein function in *Salmonella enterica* and *Saccharomyces cerevisiae*, Genetics 163 (2003) 545–555.
[25] A.A. Falcon, S. Chen, M.S. Wood, J.P. Aris, Acetyl-coenzyme A synthetase 2 is a nuclear protein required for replicative longevity in *Saccharomyces cerevisiae*, Mol. Cell. Biochem. 333 (2010) 99–108.
[26] M.A. van den Berg, P. de Jong-Gubbels, C.J. Kortland, J.P. van Dijken, J.T. Pronk, H.Y. Steensma, The two acetyl-coenzyme A synthetases of *Saccharomyces cerevisiae* differ with respect to kinetic properties and transcriptional regulation, J. Biol. Chem. 271 (1996) 28953–28959.
[27] A. Baudin, O. Ozier-Kalogeropoulos, A. Denouel, F. Lacroute, C. Cullin, A simple and efficient method for direct gene deletion in *Saccharomyces cerevisiae*, Nucleic Acids Res. 21 (1993) 3329–3330.
[28] L. Calzari, I. Orlandi, L. Alberghina, M. Vai, The histone deubiquitinating enzyme Ubp10 is involved in rDNA locus control in *Saccharomyces cerevisiae* by affecting Sir2p association, Genetics 174 (2006) 2249–2254.
[29] M. Vanoni, M. Vai, L. Popolo, L. Alberghina, Structural heterogeneity in populations of the budding yeast *Saccharomyces cerevisiae*, J. Bacteriol. 156 (1983) 1282–1291.
[30] D. Porro, L. Brambilla, L. Alberghina, Glucose metabolism and cell size in continuous cultures of *Saccharomyces cerevisiae*, FEMS Microbiol. Lett. 229 (2003) 165–171.
[31] C. Verduyn, E. Postma, W.A. Scheffers, J.P. Van Dijken, Effect of benzoic acid on metabolic fluxes in yeasts: a continuous-culture study on the regulation of respiration and alcoholic fermentation, Yeast 8 (1992) 501–517.
[32] G. Agrimi, L. Brambilla, G. Frascotti, I. Pisano, D. Porro, M. Vai, L. Palmieri, Deletion or overexpression of mitochondrial NAD^+ carriers in *Saccharomyces cerevisiae* alters cellular NAD and ATP contents and affects mitochondrial metabolism and the rate of glycolysis, Appl. Environ. Microbiol. 77 (2011) 2239–2246.
[33] E. Postma, C. Verduyn, W.A. Scheffers, J.P. Van Dijken, Enzymic analysis of the crabtree effect in glucose-limited chemostat cultures of *Saccharomyces cerevisiae*, Appl. Environ. Microbiol. 55 (1989) 468–477.
[34] D.H. Lee, A.L. Goldberg, Proteasome inhibitors cause induction of heat shock proteins and trehalose, which together confer thermotolerance in *Saccharomyces cerevisiae*, Mol. Cell. Biol. 18 (1998) 30–38.
[35] P. de Jong-Gubbels, P. Vanrolleghem, S. Heijnen, J.P. van Dijken, J.T. Pronk, Regulation of carbon metabolism in chemostat cultures of *Saccharomyces cerevisiae* grown on mixtures of glucose and ethanol, Yeast 11 (1995) 407–418.
[36] M. Vai, L. Popolo, R. Grandori, E. Lacana, L. Alberghina, The cell cycle modulated glycoprotein Gp115 is one of the major yeast proteins containing glycosylphosphatidylinositol, Biochim. Biophys. Acta 1038 (1990) 277–285.
[37] P. Ludovico, M.J. Sousa, M.T. Silva, C. Leao, M. Corte-Real, *Saccharomyces cerevisiae* commits to a programmed cell death process in response to acetic acid, Microbiology 147 (2001) 2409–2415.
[38] P. Fabrizio, V.D. Longo, The chronological life span of *Saccharomyces cerevisiae*, Methods Mol. Biol. 371 (2007) 89–95.
[39] C. Wills, D. Hom, An efficient selection producing structural gene mutants of yeast alcohol dehydrogenase resistant to pyrazole, Genetics 119 (1988) 791–795.
[40] W.C. Burhans, M. Weinberger, DNA replication stress, genome instability and aging, Nucleic Acids Res. 35 (2007) 7545–7556.
[41] M. Weinberger, A. Mesquita, T. Caroll, L. Marks, H. Yang, Z. Zhang, P. Ludovico, W.C. Burhans, Growth signaling promotes chronological aging in budding yeast by inducing superoxide anions that inhibit quiescence, Aging 2 (2010) 709–726.
[42] C.J. Murakami, V. Wall, N. Basisty, M. Kaeberlein, Composition and acidification of the culture medium influences chronological aging similarly in vineyard and laboratory yeast, PLoS One 6 (2010) e24530.
[43] I. Orlandi, N. Casatta, M. Vai, Lack of Ach1 CoA-transferase triggers apoptosis and decreases chronological lifespan in yeast, Front. Oncol. 2 (2012) 67, http://dx.doi.org/10.3389/fonc.2012.00067.
[44] M. Casal, H. Cardoso, C. Leao, Effects of ethanol and other alkanols on transport of acetic acid in *Saccharomyces cerevisiae*, Appl. Environ. Microbiol. 64 (1998) 665–668.
[45] M. Mollapour, P.W. Piper, Hog1 mitogen-activated protein kinase phosphorylation targets the yeast Fps1 aquaglyceroporin for endocytosis, thereby rendering cells resistant to acetic acid, Mol. Cell. Biol. 27 (2007) 6446–6456.
[46] J.T. Pronk, Auxotrophic yeast strains in fundamental and applied research, Appl. Environ. Microbiol. 68 (2002) 2095–2100.
[47] A. Kolkman, P. Daran-Lapujade, A. Fullaondo, M.M. Olsthoorn, J.T. Pronk, M. Slijper, A.J. Heck, Proteome analysis of yeast response to various nutrient limitations, Mol. Syst. Biol. 2 (2006) 2006–2026.
[48] M.T. Kresnowati, C.M. Suarez-Mendez, W.A. van Winden, W.M. van Gulik, J.J. Heijnen, Quantitative physiological study of the fast dynamics in the intracellular pH of *Saccharomyces cerevisiae* in response to glucose and ethanol pulses, Metab. Eng. 10 (2008) 39–54.
[49] D. Visser, G.A. van Zuylen, J.C. van Dam, M.R. Eman, A. Proll, C. Ras, L. Wu, W.M. van Gulik, J.J. Heijnen, Analysis of *in vivo* kinetics of glycolysis in aerobic *Saccharomyces cerevisiae* by application of glucose and ethanol pulses, Biotechnol. Bioeng. 88 (2004) 157–167.
[50] M.M. dos Santos, A.K. Gombert, B. Christensen, L. Olsson, J. Nielsen, Identification of *in vivo* enzyme activities in the cometabolism of glucose and acetate by *Saccharomyces cerevisiae* by using 13C-labeled substrates, Eukaryot. Cell 2 (2003) 599–608.
[51] P. de Jong-Gubbels, M.A. van den Berg, M.A. Luttik, H.Y. Steensma, J.P. van Dijken, J.T. Pronk, Overproduction of acetyl-coenzyme A synthetase isoenzymes in respiring *Saccharomyces cerevisiae* cells does not reduce acetate production after exposure to glucose excess, FEMS Microbiol. Lett. 165 (1998) 15–20.
[52] F. Remize, E. Andrieu, S. Dequin, Engineering of the pyruvate dehydrogenase bypass in *Saccharomyces cerevisiae*: role of the cytosolic $Mg(2+)$ and mitochondrial $K(+)$ acetaldehyde dehydrogenases Ald6p and Ald4p in acetate formation during alcoholic fermentation, Appl. Environ. Microbiol. 66 (2000) 3151–3159.
[53] Y.Y. Lin, J.Y. Lu, J. Zhang, W. Walter, W. Dang, J. Wan, S.C. Tao, J. Qian, Y. Zhao, J.D. Boeke, S.L. Berger, H. Zhu, Protein acetylation microarray reveals that NuA4 controls key metabolic target regulating gluconeogenesis, Cell 136 (2009) 1073–1084.
[54] L. Shi, B.M. Sutter, X. Ye, B.P. Tu, Trehalose is a key determinant of the quiescent metabolic state that fuels cell cycle progression upon return to growth, Mol. Biol. Cell 21 (2010) 1982–1990.
[55] V.D. Longo, G.S. Shadel, M. Kaeberlein, B. Kennedy, Replicative and chronological aging in *Saccharomyces cerevisiae*, Cell Metab. 16 (2012) 18–31.